Photodegradation of Sulfonylurea Molecules: Analytical and Theoretical DFT Studies

Clémence Corminboeuf,[†] Fabrice Carnal,[†] Jacques Weber,[†] Jean-Marc Chovelon,[‡] and Henry Chermette*[,§]

Department of Physical Chemistry, University of Geneva, 30 quai Ernest-Ansermet, CH-1211, Genève 4, Switzerland, Laboratoire d'Application de la Chimie à l'Environnement, LACE, UMR 5634, Université Claude Bernard Lyon-1, 43 Bd du 11 novembre 1918, Villeurbanne Cedex, France, and Laboratoire de Chimie Physique Théorique, bât 210, Université Claude Bernard Lyon-1 and UMR CNRS 5182, 43 bd du 11 novembre 1918, 69622-Villeurbanne Cedex, France

Received: June 23, 2003; In Final Form: September 1, 2003

The use and the number of sulfonylurea herbicides have increased since the early 1980s. A good understanding of their degradation is of ecological importance, since environmental pollutants can be issued from them. It is claimed that microbial degradation and chemical hydrolysis present the main degradation pathways but photodegradation cannot be neglected. Time-dependent density functional theory has been used to help in the elucidation of the photochemical behavior of sulfonylureas.

Introduction

Herbicides belong to an important class of organic chemicals. They are abundantly used in agriculture, since they improve productivity, but they increase environmental pollution as well. Nowadays, researchers are looking for compounds which are ecologically safer.

Sulfonylurea herbicides were, for example, discovered in the middle of the 1970s[1] and have become widely used due to their low application rates (∼2−75 g/ha), good crop selectivity, and very low animal toxicity.[2,3] However, depending on environmental conditions, sulfonylurea may persist excessively in the environment with residual phytotoxicity. For this reason a better knowledge of their degradation is required.

Sulfonylureas are composed of three distinct parts: a triazine derivative, a benzene derivative, and a sulfonylurea bridge.[2,4]

According to experiment,[5,6] the photodegradation of the sulfonylurea molecules occurs at irradiation wavelengths < 300 nm. A complementary study using molecular modeling should help in the understanding of the photochemical behavior and also in the forecast of the photodegradation mechanisms.

Consequently, this paper reports the theoretical study of the photodissociation of the S−X bonds (X = C, N) and the molecular orbitals involved in the degradation process of two sulfonylureas: the chlorosulfuron and a derivative of the cinosulfuron (see Figure 1).

Density functional theory (DFT)[7] has been applied for the purpose, and the theoretical prediction of the bond breaking of an electronically excited compound has been obtained through a geometry optimization of the monodeterminantal monoelectronic DFT excited state. It seems realistic, since it is contrary to the Hartree−Fock or semiempirical Hamiltonians, that most of the electronic correlation present in the excited state is already brought about by the exchange-correlation functional. One knows, however, that this is exactly true only for the lowest state of a given symmetry,[8] but this remains pragmatically true for most of the low-energy states, as has been proved for a while through more than 20 years of calculations.[9]

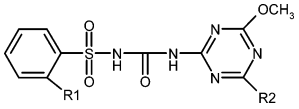

Figure 1. (a) R1 = R2 = OCH_3, shortened cinosulfuron; (b) R1 = $OCH_2CH_2OCH_3$, R2 = OCH_3, cinosulfuron; (c) R1 = Cl, R2 = CH_3, chlorosulfuron; (d) R1 = OCH_2CH_2Cl, R2 = CH_3, triasulfuron.

Computational Details

Density functional theory (DFT) calculations have been performed to optimize the geometries of the studied molecules, to give an assignment to the UV/VIS spectrum, and to obtain the geometries of the (photo)excited states. The latter can be either slightly different from the ground-state structure or split into two fragments resulting from a photoinduced bond cleavage. The nature of these fragments will then be compared to experimental analysis. Ground-state geometry optimizations have been performed using various exchange-correlation (XC) functionals (LDA,[10] PW91,[11] and B88P86[12,13]) together with both Gaussian orbitals[14] and Slater type orbitals,[15] complemented by comparison with X-ray data. To save computational time, the R1 group present in cinosulfuron has been reduced to a methoxy group, but further calculations on the entire molecule showed that this simplification does not influence the spectrum. Absorption spectra have been calculated using time-dependent DFT[16,17] (TD-DFT), based on the linear and nonlinear response formalism,[18] and calculation of the excitation energies with the iterative Davidson procedure[19] as implemented in the ADF program.[15] Two functionals, namely the van Leeuwen−Baerends[20] (LB94) and the recently implemented SAOP[21] by Gritsenko, Schipper, and Baerends, based on a statistical averaging of (model) orbital potentials have been used. Unlike standard functionals, those functionals possess a correct asymptotic 1/*r* behavior and lead to a better estimation of the high-energy part

* To whom correspondence should be addressed. E-mail: Henry.Chermette@univ-lyon1.fr,cherm@in2p3.fr.
† University of Geneva. E-mail: clemence.corminboeuf@chiphy.unige.ch.
‡ Laboratoire d'Application de la Chimie à l'Environnement, LACE, UMR 5634, Université Claude Bernard Lyon-1.
§ Laboratoire de Chimie Physique Théorique, bât 210, Université Claude Bernard Lyon-1 and UMR CNRS 5182.

10.1021/jp035776b CCC: $25.00
Published on Web 11/01/2003

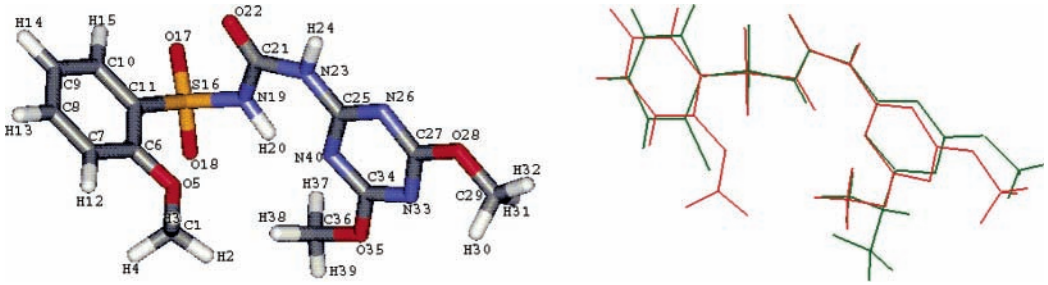

Figure 2. (a, left) Atom numbering and (b, right) structure matching of a derivative of cinosulfuron at the PW91/DZVP level (red) and an experimental structure (green).[22]

TABLE 1: Geometrical Parameters of a Derivative of Cinosulfuron at Different Levels of Theory

		ADF 2002		Gaussian 98		
geometry	X-ray	PW91 TZP	B88P86 TZP	SVWN5/DZVP	PW91 6-31G**	PW91 DZVP
lengths						
C6−C11	1.384	1.420	1.416	1.407	1.416	1.418
C11−S16	1.758	1.816	1.788	1.771	1.795	1.801
S16−N19	1.634	1.727	1.696	1.686	1.715	1.720
N19−C21	1.372	1.386	1.379	1.371	1.380	1.380
angles						
C10−C11−S16	117.1	117.4	117.5	118.0	117.6	117.3
C11−S16−N19	104.1	105.8	105.6	103.0	104.2	104.2
S16−N19−C21	123.3	126.6	126.8	122.5	124.4	125.0
N19−C21−N23	115.4	114.0	113.3	112.9	113.3	113.7
C21−N23−C25	130.8	132.6	132.0	129.0	131.5	131.6
C27−O28−C29	117.7	117.8	117.2	116.6	116.9	117.0
N26−C27−O28	113.5	119.6	119.2	118.3	118.7	118.9
dihedral angles						
C10−C11−S16−N19	102.7	123.0	122.0	122.8	125.0	121.7
C11−S16−N19−C21	−69.1	−60.0	−67.3	−49.3	−52.9	−56.5
S16−N19−C21−N23	−177.9	167.6	178.8	156.6	165.8	173.1
N19−C21−N23−C25	1.0	−9.3	−3.5	−18.1	−11.5	−6.1
N26−C27−O28−C29	−172.3	−0.3	−0.7	−1.3	−0.6	−0.5
O17−S16−N19−C21	45.4	55.6	48.0	65.5	62.1	58.3
O22−C21−N23−C25	−179.4	171.5	176.5	161.6	168.8	173.9
C10−C11−S16−O18	−144.6	−127.6	−128.7	−128.8	−125.9	−129.1
C11−C6−O5−C1		177.8	−180.0	176.9	179.1	−179.1
N33−C34−O35−C36		−176.9	−177.5	−179.1	−178.0	178.1

of the absorption bands. A triple-ζ plus one polarization function (TZP, previously denoted set IV) basis set has been used. Moreover, as recommended,[15] cores have not been kept frozen when calculating the SAOP transitions. The most intense transition energies can be assigned to a dominant monoelectronic transition between two Slater determinants. Further, the geometry of the corresponding monoelectronically excited determinants has been optimized with a standard GGA[11] (PW91) XC functional. Indeed, the theoretical prediction of the bond breaking of an electronically excited compound is easy to perform using code like ADF,[15] because the orbital character is kept along the geometry optimizations of the monodeterminantal monoelectronic excited states. If not specified, singlet excited configurations were considered rather than the corresponding triplet.

Results and Discussions

Geometrical parameters of a cinosulfuron derivative are displayed in Table 1 and compared to the X-ray data[22] (see Figure 2). Several functionals and basis sets have been tested. As expected, LDA bond lengths are shorter than GGA ones and closer to experiment. However, the dihedral angles obtained with the local density approximation are less satisfying. The PW91/DZVP geometry obtained with Gaussian 98[14] shows the best agreement with experiment (see Figure 2b) and has therefore been used for the time-dependent DFT study, as well as for the geometry optimization of the chlorosulfuron. In particular, a very similar geometry has been obtained using the B3LYP functional: the most important bond lengths in this work, namely the S−N and the S−C bond lengths, differ by less than 0.02 and 0.01 Å, respectively, with respect to the used PW91/DZVP geometry. These values, which are very close to the B88P86 ones (see Table 1), are too small to induce differences in bond breaking properties.

The experimental spectra of both molecules exhibit three significant features:[5,6] The benzene-like band below 300 nm, the triazine-centered shoulder between 240 and 260 nm, and the most intense band with a maximum at 220 and 195 nm for chlorosulfuron and cinosulfuron, respectively. These features, which show transitions between orbitals localized on either the benzene skeleton or the triazine group, also confirm that the two chromophores (benzene derivative and triazine group) are weakly coupled in these molecules. Figure 3 and Tables 2S and 3S (full theoretical spectra tables are given in the Supporting Information) show the calculated UV absorption transitions of the two molecules using the LB94 and SAOP potentials, whereas Tables 2 and 3 only display the transitions implying the molecular orbitals playing a major role during the dissociation (see next section).

It can be underlined that the SAOP functional leads to a theoretical spectrum which is closer to experiment than that of the LB94 functional. This was expected since the SAOP functional has been developed later than the LB94 functional with the goal to predict more accurately electronic spectra.

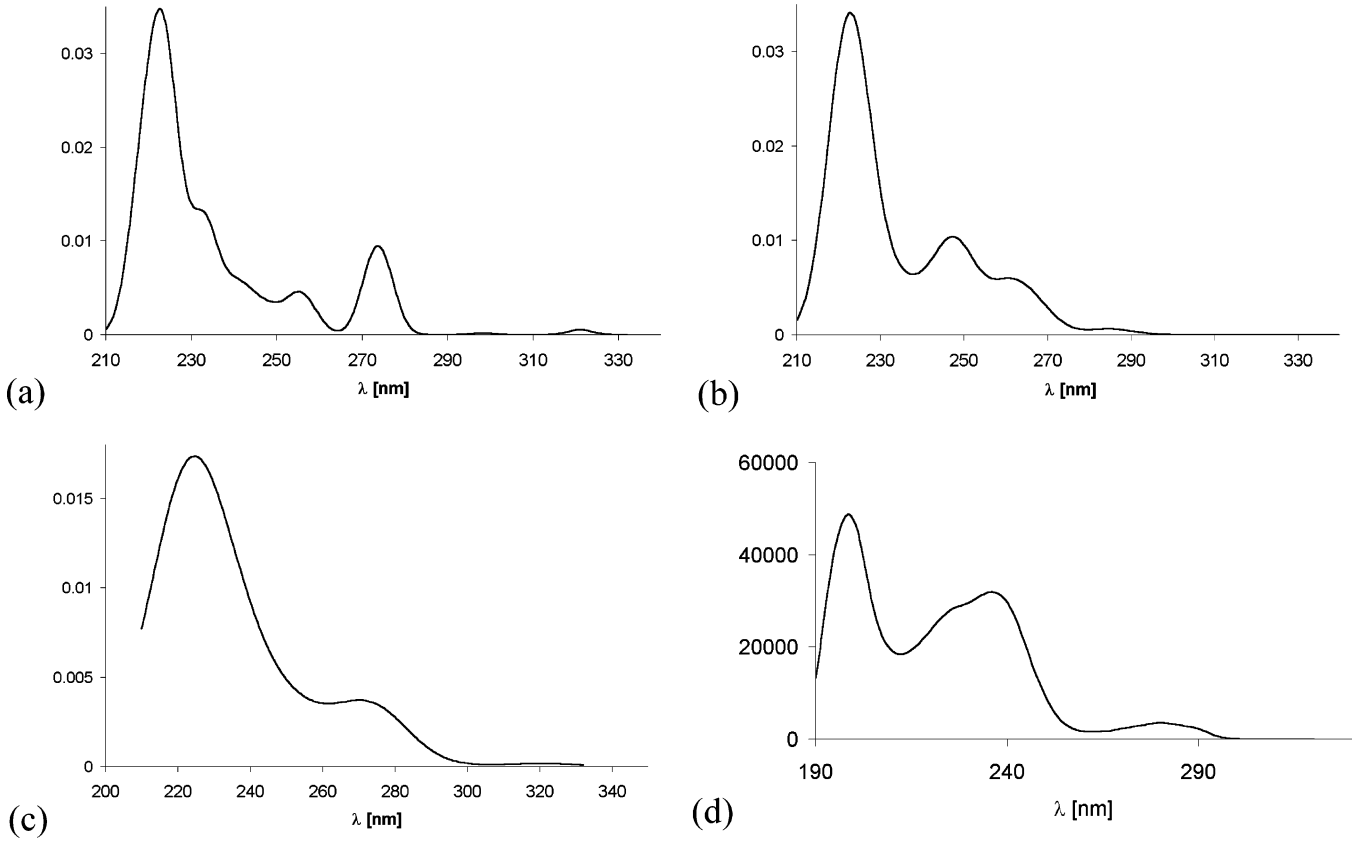

Figure 3. Graphical representation of the absorption spectrum of (a and c) cinosulfuron at the SAOP/TZP level and (b) chlorosulfuron at the (SAOP/TZP) level and (d) the experimental spectrum of cinosulfuruon. The theoretical peaks are convoluted by a sum of 5 nm Gaussian functions (fwhm) for parts a and b and 10 nm functions for part c.

At this stage of the theoretical study, the analysis of the shape and energy of the frontier orbitals of each studied molecule is necessary to get a better understanding of the role played by these molecular orbitals during the photodissociation. In the coming section, these detailed pieces of information are treated separately for the two molecules.

(a) Chlorosulfuron. As described by Caselli et al.,[5] absorption at 254 nm by the triazine chromophore in chlorosulfuron results in energy transfer to the sulfonylurea bridge and subsequent competitive cleavage reactions. The major products identified result from the photodissociation of the S−N bond. Theoretical transitions involving the LUMO+2, whose orbital analysis shows the presence of charge density on both the triazine and the sulfonyl bridge, have therefore been considered in the study of the photodegradation mechanism. The relaxation of the geometry of the chlorosulfuron molecule when raising one electron from the HOMO-4 to LUMO+2 leads to the cleavage of the S−N bond. As shown in Figure 4, this corresponds to the excitation of the triazine chromophore.

As already mentioned above, the experimental cleavage of the S−N bond was produced upon an irradiation at 254 nm. This value is within the theoretical excitation energy range obtained with the LB94 (263.2 nm) and the SAOP (240 nm) levels of calculation (see Table 3), so that the results can be considered as in good agreement with experiment.

(b) Cinosulfuron. The same study has been carried out on the derivative of cinosulfuron. As can be shown by comparing Figures 4 and 5, the orbitals of the two molecules are relatively close in shape, but important differences can be observed: The HOMO-1 and the LUMO of Figure 5 appear to be slightly delocalized over the benzene moiety, which is not the case for the chlorosulfuron. Also, the electronic density on the sulfonyl bridge of chlorosulfuron is mainly located on the LUMO+1 and LUMO+2, while, in the case of the cinosulfuron, it involves mostly the LUMO and LUMO+1. For these reasons, it is not necessarily expected that the same transitions would induce the same bond dissociation. Transitions to the LUMO, strongly localized on the triazine and on the sulfonyl bridge, have thus been theoretically investigated. As shown in Figure 5, the monoelectronic excitation HOMO-1 → LUMO followed by a geometry relaxation leads to the cleavage of the S−N bond. The energy transition obtained using SAOP/TZP (272.15 nm) is once again 20 nm lower than the one obtained using LB94/IV (298.6 nm) (see Table 2). The experimental band[5,6] corresponding to the absorption of the triazine chromophore covers a large region of the spectrum (215−270 nm), but the cleavage of the nitrogen−sulfur bond is said to be far less important than the carbon−sulfur cleavage.[6] In fact, in ref 6 the minor S−N dissociation follows an excitation with a wavelength of 290 nm in aqueous medium, which does not allow an efficient excitation of the triazine absorption band and can explain the weak importance of the S−N dissociation.

Actually, the main photoproduct issued from cinosulfuron described by Chovelon et al.[6] is $HO_3SHNCONH-$triazine, which has been interpreted as resulting from the carbon−sulfur cleavage. Pusino et al., using triasulfuron, a sulfonylurea herbicide very close to cinosulfuron (see Figure 1d), have drawn similar conclusions.[23] In both cases, the photodegradation experiments were performed in aqueous solution (100% water for Chovelon et al. and 49/51 acetonitrile/water for Pusino et al.). Our gas-phase calculations did not lead to this carbon−sulfur cleavage, but in a more recent study, Chovelon et al. have found[24] that, in pure acetonitrile, one obtains $H_2NCONH-$triazine as a main photoproduct resulting from a S−N, as

TABLE 2: Theoretical Absorption Spectrum of Cinosulfuron[a]

SAOP/TZP				LB94/IV			
eV	nm	oscill	MO	eV	nm	oscill	MO
3.86	321.20	4.18×10^3	HOMO → LUMO (H → L)	3.47	357.04	3.25×10^3	HOMO → LUMO
4.56*	271.89*	4.25×10^2*	H-1 → L*	4.15*	298.56*	2.39×10^2*	H-1 → L*
4.79	258.84	5.65×10^3	H-2 → L	4.25	291.52	5.55×10^3	H-2 → L
4.87	254.58	2.26×10^2	H-3 → L (38) H-2 → L+1 (22)	4.49	276.01	2.36×10^3	H-2 → L+1 (45) H-4 → L (23) H-3 → L (21)
5.03	246.49	4.78×10^3	H-4 → L	4.55	272.25	2.36×10^3	H-5 → L (47) H-2 → L+2 (32)
5.08	244.06	9.36×10^3	H-5 → L (56) H-6 → L (15)	4.57	271.39	4.50×10^3	H-2 → L+2 (53) H-5 → L (25) H-1 → L+2 (11))
5.16	240.28	1.69×10^2	H-6 → L (58) H-3 → L+2 (21)	4.65	266.54	6.83×10^2	H-6 → L (23) H-4 → L+1 (12) H-3 → L+1 (11) H-4 → L+1 (11)
5.3	233.93	2.84×10^2	H-6 → L+1 (42) H-7 → L (26)	4.83	256.51	1.78×10^2	H-7 → L (48) H-6 → L (15) H-3 → L+1 (13)
5.4	229.60	1.83×10^2	H-7 → L (29) H-5 → L+2 (12) H → L+3 (10)	4.95	250.68	2.03×10^2	H-6 → L (47) H-7 → L (14) H-6 → L+2 (14)
5.5	225.42	9.09×10^3	H-7 → L+1 (38) H-8 → L (22)	5.00	248.08	7.96×10^3	H-6 → L+2 (29) H-7 → L+1 (16) H-6 → L+1 (16) H-8 → L (12)
5.52	224.61	0.1267	H-3 → L (18) H-3 → L+1 (13)	5.07	244.49	4.94×10^2	H-7 → L+2 (25) H-4 → L+2 (11) H-7 → L (10)
5.58	222.19	7.44×10^2	H-9 → L (40) H-6 → L+2 (11)	5.13	241.88	3.23×10^2	H-9 → L (37) H-10 → L (21)
5.64	219.83	5.04×10^2	H-8 → L (29) H-9 → L (18) H-8 → L+1 (16)	5.14	241.43	6.60×10^2	H-4 → L+1 (13) H-9 → L (11) H-3 → L+1 (10) H-9 → L+1 (10) H-3 → L (10)
5.72	216.75	3.87×10^2	H-10 → L (54) H-8 → L+1 (14) H → L+4 (12)	5.18	239.48	4.27×10^2	H-10 → L
				5.30	233.84	5.23×10^2	H-8 → L+1 (39) H-9 → L+1 (14) H-10 → L (10)
				5.32	232.95	9.39×10^2	H-10 → L (18) H-8 → L (12)

[a] The oscillator strength and the major assignation(s) (>10%, in parentheses) are given for each monoelectronic transition (energy in eV, wavelength in nm) implying the LUMO (L) (see text). Transitions leading to dissociation are marked with asterisks. [H = HOMO]

obtained by calculations. This suggests that the observed photoproducts as well as the photodegradation pathway depend strongly on experimental conditions and may involve complex mechanisms. It is therefore likely that the gas-phase calculations do not lead to the cleavage of this bond, observed in aqueous medium, because of the absence of important solvent interactions, not taken into account in our model. A preliminary transformation of the molecule through interaction with an acidic medium may also be considered, and work in this direction is in progress.

One has to emphasize that the isolation of 2-chloroethoxybenzene from the triasulfuron may result either by an S−C bond cleavage, as suggested by Pusino et al.,[23] or by the S−N bond cleavage followed by the abstraction of SO_2 from the sulfonylchloroethoxybenzene moiety. Indeed, no experimental evidence of a (4-methoxy-6-methyl-1,3,5,triazine-2-yl)sulfonylurea has been found in Pusino's work, since only the (4-methoxy-6-methyl-1,3,5-triazine-2-yl)urea has been isolated, indicating that the S−N bond may be easily broken. Therefore, we suggest the formation of a sulfonylchloroethoxybenzene intermediate, followed by a sulfur dioxide loss leading to the chloroethoxybenzene photoproduct. The acidic character of the abstracted SO_2 molecule will induce an enhanced sensitivity to the solvent nature.

It is also worth noting that calculations taking into account either the first excited singlet state or the lowest excited triplet state did allow us to reach the same conclusions, namely the absence of the carbon−sulfur bond cleavage.

Influence of the Ortho Substituents on the Photodissociation. Another aspect that should be discussed here concerns the influence of the ortho substituent group on the photodissociation. As can be shown by our results (Figure 3 and Tables 2 and 3), an ortho oxygen substituent red-shifts the triazine and benzene absorption bands. This induces a weakening of the S−N cleavage in comparison to the case of the molecule containing a chlorine. According to Yang et al.[25] the ortho chloro group attached to the benzene also reinforces the photochemical stability of the C−S bond, which would explain the absence of this kind of dissociation in the experimental photodegradation of the chlorosulfuron molecule. The choice of the ortho group could have therefore an important ecological impact.

TABLE 3: Theoretical Absorption Spectrum of Chlorosulfuron[a]

SAOP/TZP				LB94/IV			
eV	nm	oscil	MO	eV	nm	oscil	MO
4.29	288.89	2.25×10^3	H → L+2 (70) H → L+1 (29)	4.33	286.65	1.43×10^2	H-2 → L+1 (63) H-1 → L+2 (28)
4.65	266.53	1.73×10^2	H-2 → L+1 (31) H → L+1 (31) H → L+2 (16)	4.35	285.13	6.40×10^3	H-1 → L+2 (34) H-6 → L (29) H → L+2 (19)
4.74	261.72	6.27×10^3	H-4 → L (72) H-1 → L+2 (11)	4.35	284.91	1.36×10^2	H → L+2 (43) H-6 → L (27)
4.75	260.81	4.19×10^2	H-1 → L+2 (36) H-1 → L+1 (19)	4.38	282.85	1.49×10^2	H-1 → L+2 (29) H-6 → L (28) H-2 → L+1 (20)
4.84	256.28	7.20×10^3	H-5 → L	4.65	266.67	3.44×10^2	H-5 → L+2 (38) H-8 → L (14) H-6 → L+1 (12)
4.90	252.85	9.55×10^3	H-6 → L (48) H-3 → L (16) H-7 → L (14)	4.69	264.17	3.34×10^3	H-8 → L (35) H-4 → L+2 (28) H-5 → L+2 (11)
4.93	251.62	2.04×10^3	H-2 → L+2 (65) H-5 → L+1 (14)	4.71*	263.19*	3.33×10^2*	H-4 → L+2 (36)* H-6 → L+1 (18) H-8 → L (17)
5.00	248.18	1.27×10^2	H-2 → L+2	4.81	257.80	8.83×10^3	H-6 → L+2 (54) H-7 → L+1 (11)
5.17*	240.00*	4.84×10^3*	H-4 → L+2 (61)* H-5 → L+2 (18)*	4.84	256.23	2.95×10^2	H-7 → L (33) H-6 → L+2 (32)
5.23	236.96	1.35×10^2	H-5 → L+2 (34) H-8 → L+1 (21) H-4 → L+2 (17)	4.90	253.09	2.86×10^2	H-7 → L (17) H-2 → L+2 (13) H-7 → L+2 (12) H-9 → L+1 (10)
5.31	233.43	1.25×10^2	H-5 → L+2 (27) H-6 → L+1 (27) H-6 → L+2 (10)	4.99	248.36	1.26×10^2	H-7 → L+2 (45) H-8 → L+2 (33)
5.45	227.54	2.11×10^3	H-7 → L+2 (32) H-6 → L+2 (23) H-4 → L+3 (11)	5.05	245.61	1.55×10^2	H-6 → L+2 (21) H-6 → L+1 (16) H-5 → L+1 (12)
5.55	223.22	0.1373	H-6 → L+2 (27) H-8 → L+2 (23) H-3 → L+2 (20)				
5.58	222.27	9.23×10^2	H-6 → L+3 (52) H-3 → L+2 (16) H-8 → L+2 (11)				
5.59	221.64	0.1576	H-8 → L+2 (46) H-3 → L+2 (19)				

[a] The oscillator strength and the major assignation(s) (>10%, in parentheses) are given for each monoelectronic transition (energy in eV, wavelength in nm) implying the LUMO+2 (see text). Transitions leading to dissociation are marked with asterisks.

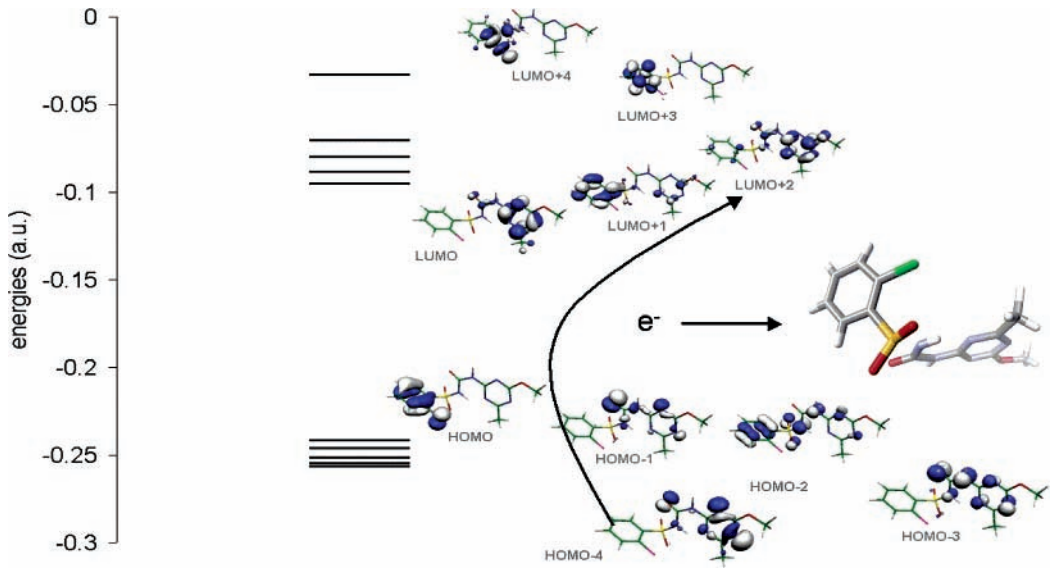

Figure 4. Scheme of the frontier orbitals of chlorosulfuron.

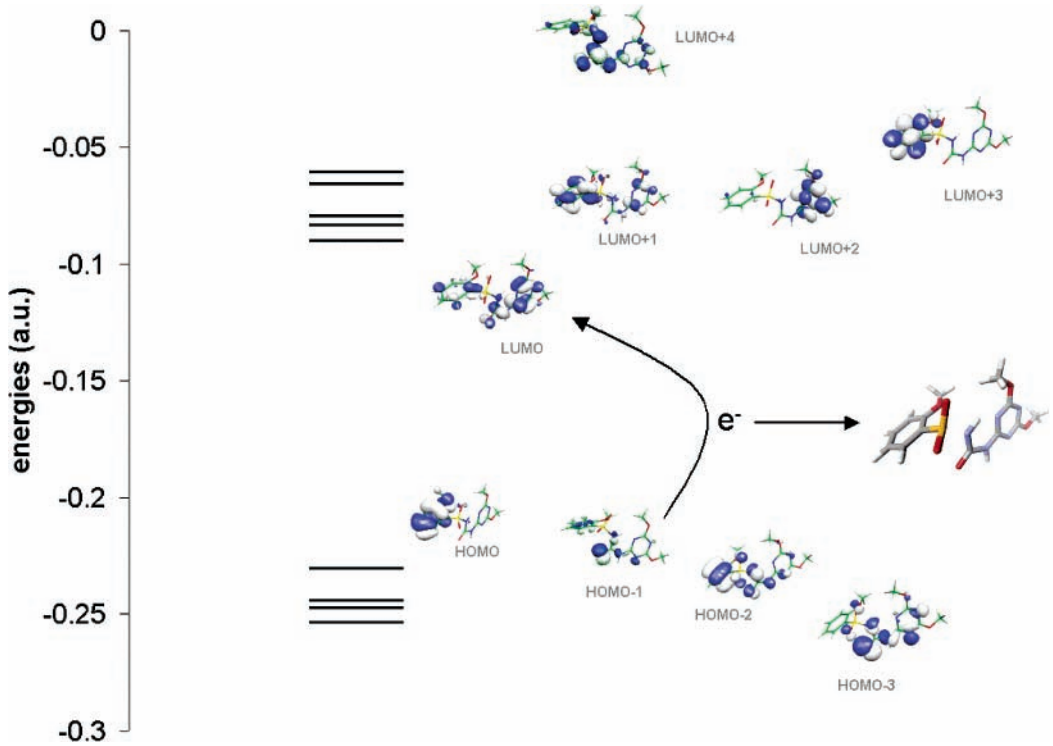

Figure 5. Scheme of the frontier orbitals of cinosulfuron.

Concluding Remarks

Analyses of experimental results on the photochemical degradation of sulfonylurea have been achieved using DFT and TD-DFT methods.

The theoretical UV spectrum has been simulated at the LB94/TZP and SAOP/TZP levels of theory. Molecular frontier orbitals have been analyzed in order to select those involved in the photochemical degradation process.

The transitions occurring in the degradation process were determined by taking into account the orbital characters, the calculated transitions, and the experimental energies. It has been shown that the HOMO-1 to LUMO monoelectronic excitation implies the cleavage of the sulfur−nitrogen bond in the cinosulfuron, whereas the HOMO-4 → LUMO+2 excitation induces the same dissociation in chlorosulfuron. The influence of the ortho substituent on the dissociation has also been demonstrated.

The theoretical rupture of the carbon−sulfur bond in cinosulfuron has not been predicted, which indicates that a more complex mechanism might be involved.

Obtaining the S−N or S−C bond cleavage through a theoretical photochemical excitation is a powerful approach to model the ecological properties of phytosanitary compounds. However, the exact degradation process may be more complex, for example, when no significant localization of involved atomic orbitals is obtained or when other factors such as acidity or solvent interactions may play a significant role in the process. Analysis of all these factors is currently under investigation.

Acknowledgment. This work is a part of Project 20-63496.00/1 of the Swiss National Foundation. The CINES is acknowledged for a grant of computer time (Project cpt2130).

Supporting Information Available: Full theoretical spectra tables of cinosulfuron and chlorosulfuron. This material is available free of charge via the Internet at http://pubs.acs.org.

References and Notes

(1) Levitt, G.; Ploeg, H. L.; Hans, L.; Weigel, R. C.; Fitzgerald, D. J. *J. Agric. Food Chem.* **1981**, *29*, 416.
(2) Brown, H. M. *Pestic. Sci.* **1990**, *29*, 263.
(3) Blair, A. M.; Martin, T. D. *Pestic. Sci.* **1988**, *22*, 195.
(4) Beyer. In *Herbicides: chemistry degradation and mode of actions*; Kearney, P. C., Kaufmann, D. D., Eds.; Marcel Dekker: New York, 1988; Vol. 3.
(5) Caselli, M.; Ponterini, G.; Vignali, M. *J. Photochem. Photobiol., A* **2001**, *138*, 129.
(6) Vuillet, E.; Emmelin, C.; Grenier-Loustallot, M. F.; Païssé, O.; Chovelon, J. M. *J. Agric. Food. Chem.* **2002**, *50*, 1081.
(7) Koch, W.; Holthausen, M. C. *A Chemist's Guide to Density Functional Theory*; Wiley-VCH: Weinheim, 2000. Parr, R. G.; Yang, W. *Density Functional Theory of Atoms and Molecules*; Oxford University Press: New York, 1989.
(8) (a) Von Barth, U. *Phys. Rev. A* **1979**, 20, 1693. (b) Gunnarson, O.; Lundqvist, B. I. *Phys. Rev. B* **1976**, *13*, 4274.
(9) Chermette, H. *Coord. Chem. Rev.* **1998**, *178*, 699.
(10) Vosko, S. H.; Wilk, L.; Nusair. *Can. J. Phys.* **1980**, *58*, 1200.
(11) Perdew, J. P.; Wang, Y. In *Electronic Structure of Solids'91*; Ziesche, P., Eschrig, H., Eds.; Academie Verlag: Berlin, 1991; p 11.
(12) Becke, A. D. *Phys. Rev. A* **1988**, *38*, 3098.
(13) Perdew, J. P. *Phys Rev. B* **1986**, *33*, 8822.
(14) Frisch, M. J.; Trucks, G. W.; Schlegel, H. B.; Scuseria, G. E.; Robb, M. A.; Cheeseman, J. R.; Zakrzewski, V. G.; Montgomery, J. A., Jr.; Stratmann, R. E.; Burant, J. C.; Dapprich, S.; Millam, J. M.; Daniels, A. D.; Kudin, K. N.; Strain, M. C.; Farkas, O.; Tomasi, J.; Barone, V.; Cossi, M.; Cammi, R.; Mennucci, B.; Pomelli, C.; Adamo, C.; Clifford, S.; Ochterski, J.; Petersson, G. A.; Ayala, P. Y.; Cui, Q.; Morokuma, K.; Malick, D. K.; Rabuck, A. D.; Raghavachari, K.; Foresman, J. B.; Cioslowski, J.; Ortiz, J. V.; Baboul, A. G.; Stefanov, B. B.; Liu, G.; Liashenko, A.; Piskorz, P.; Komaromi, I.; Gomperts, R.; Martin, R. L.; Fox, D. J.; Keith, T.; Al-Laham, M. A.; Peng, C. Y.; Nanayakkara, A.; Gonzalez, C.; Challacombe, M.; Gill, V.; Johnson, B. G.; Chen, W.; Wong, M. W.; Andres, J. L.; Head-Gordon, M.; Replogle, E. S.; Pople, J. A. *Gaussian 98*, Revision A.8; Gaussian, Inc.: Pittsburgh, PA, 1998.
(15) Baerends, E. J.; Autschbach, J. A.; Bérces, A.; Bo, C.; Boerrigter, P. M.; Cavallo, L.; Chong, D. P.; Deng, L.; Dickson, R. M.; Ellis, D. E.; Fan, L.; Fischer, T. H.; Fonseca Guerra, C.; van Gisbergen, S. J. A.; Groeneveld, J. A.; Gritsenko, O. V.; Grüning, M.; Harris, F. E.; van den Hoek, P.; Jacobsen, H.; van Kessel, G.; Kootstra, F.; van Lenthe, E.; Osinga, V. P.; Patchkovskii, S.; Philipsen, P. H. T.; Post, D.; Pye, C. C.; Ravenek, W.; Ros, P.; Schipper, P. R. T.; Schreckenbach, G.; Snijders, J. G.; Sola, M.; Swart, M.; Swerhone, D.; te Velde, G.; Vernooijs, P.; Versluis, L.; Visser, O.; van Wezenbeek, E.; Wiesenekker, G.; Wolff, S. K.; Woo, T.

K.; Ziegler, T. ADF**2002**.03, SCM, Theoretical Chemistry, Vrije Universiteit, Amsterdam, The Netherlands, http://www.scm.com.

(16) Runge, E.; Gross, E. K. U. *Phys. Rev. Lett.* **1984**, *52*, 997.

(17) Gross, E. K. U.; Kohn, W. *Phys. Rev. Lett.* **1985**, *55*, 2850; *57*, 923.

(18) (a) van Gisbergen, S. J. A.; Snijders, J. G.; Baerends, E. *J. Comput. Phys. Commun*. **1999**, *118*, 119. (b) Jamorski, C.; Casida, M. E.; Salahub, D. R. *J. Chem. Phys.* **1996**, *104*, 5134. (c) van Gisbergen, S. J. A.; Kootstra, F.; Schipper, P. R. T.; Gritsenko, O. V.; Snijders, J. G.; Baerends, E. J. *Phys. Rev. A* **1998**, *57*, 2556.

(19) Davidson, E. R. *J. Comput. Chem.* **1975**, *17*, 87.

(20) van Leeuwen, R.; Baerends, E. J. *Phys. Rev. A* **1994**, *49*, 2421.

(21) (a) Gritsenko, O. V.; Schipper, P. R. T.; Baerends, E. J. *Int. J. Quantum Chem.* **2000**, *76*, 407. (b) Gritsenko, O. V.; Schipper, P. R. T.; Baerends, E. J. *Chem. Phys. Lett.* **1999**, *302*, 199.

(22) CCDC-VORBAF contains the crystallographic data.

(23) Pusino, A.; Braschi, I.; Petretto, S.; Gessa, C. *Pestic. Sci.* **1999**, *55*, 479.

(24) Chovelon, J. Unpublished results.

(25) Yang, X.; Wang, X.; Kong, L.; Wang, L. *Pestic. Sci.* **1999**, *55*, 479.